

Choroid Plexus Calcification Correlates with Cortical Microglial Activation in Humans: A Multimodal PET, CT, MRI Study

T. Butler, X.H. Wang, G.C. Chiang, Y. Li, L. Zhou, K. Xi, N. Wickramasuriya, E. Tanzi, E. Spector, I. Ozsahin, X. Mao, Q.R. Razlighi, E.K. Fung, J.P. Dyke, T. Maloney, A. Gupta, A. Raj, D.C. Shungu, P.D. Mozley, H. Rusinek, and L. Glodzik



ABSTRACT

BACKGROUND AND PURPOSE: The choroid plexus (CP) within the brain ventricles is well-known to produce cerebrospinal fluid (CSF). Recently, the CP has been recognized as critical in modulating inflammation. MRI-measured CP enlargement has been reported in neuroinflammatory disorders like MS as well as with aging and neurodegeneration. The basis of MRI-measured CP enlargement is unknown. On the basis of tissue studies demonstrating CP calcification as a common pathology associated with aging and disease, we hypothesized that previously unmeasured CP calcification contributes to MRI-measured CP volume and may be more specifically associated with neuroinflammation.

MATERIALS AND METHODS: We analyzed 60 subjects (43 healthy controls and 17 subjects with Parkinson's disease) who underwent PET/CT using ¹¹C-PK11195, a radiotracer sensitive to the translocator protein expressed by activated microglia. Cortical inflammation was quantified as nondisplaceable binding potential. Choroid plexus calcium was measured via manual tracing on low-dose CT acquired with PET and automatically using a new CT/MRI method. Linear regression assessed the contribution of choroid plexus calcium, age, diagnosis, sex, overall volume of the choroid plexus, and ventricle volume to cortical inflammation.

RESULTS: Fully automated choroid plexus calcium quantification was accurate (intraclass correlation coefficient with manual tracing = .98). Subject age and choroid plexus calcium were the only significant predictors of neuroinflammation.

CONCLUSIONS: Choroid plexus calcification can be accurately and automatically quantified using low-dose CT and MRI. Choroid plexus calcification—but not choroid plexus volume—predicted cortical inflammation. Previously unmeasured choroid plexus calcium may explain recent reports of choroid plexus enlargement in human inflammatory and other diseases. Choroid plexus calcification may be a specific and relatively easily acquired biomarker for neuroinflammation and choroid plexus pathology in humans.

ABBREVIATIONS: AD = Alzheimer disease; BMI = body mass index; BPnd = nondisplaceable binding potential; CP = choroid plexus; HU = Hounsfield units; ICC = intraclass correlation coefficient; PD = Parkinson disease; PK = ¹¹C-PK11195; TSPO = translocator protein

The choroid plexus (CP), a highly vascularized filamentous structure within the brain ventricular system, is well-known to produce CSF. Recently, additional, important CP functions

have been recognized, including the regulation of inflammation. The CP both initiates and modulates neuroinflammation, and CP dysfunction is considered highly relevant to the pathophysiology of disorders characterized by excess inflammation such as MS¹⁻⁶ and Alzheimer disease (AD)⁷⁻⁹ as well as normal aging.¹⁰

Unlike virtually all brain parenchymal structures, which atrophy in association with aging and dysfunction, CP enlargement appears to be pathologic, and recent MRI studies have demonstrated larger CP volume in patients with neuropsychiatric disorders, including MS,⁴⁻⁶ AD,^{7,8} depression,¹¹ and stroke,¹² and normal aging.¹⁰ The basis of CP enlargement remains uncertain, but on the basis of postmortem and animal studies, it has been posited to relate to CP basement membrane thickening and fibrous stroma expansion with protein, inflammatory cells, and deposition of metal, in particular calcium.¹³⁻¹⁶ While most of these CP components are detectable and quantifiable only through direct examination of tissue, the assessment of calcium using in

Received January 11, 2023; accepted after revision May 4.

From the Brain Health Imaging Institute (T.B., X.H.W., G.C.C., Y.L., L.Z., K.X., N.W., E.T., E.S., I.O., X.M., Q.R.R., T.M., A.G., L.G.), and Department of Radiology (X.M., E.K.F., J.P.D., D.C.S., P.D.M.), Weill Cornell Medicine, New York, New York; Department of Radiology (A.R.), University of California, San Francisco, San Francisco, California; and Department of Radiology (H.R.), New York University, New York, New York.

This work was funded by National Institutes of Health grants K23NS057579, R01NS105541, R01NS092802, R01AG072753 and a Department of Defense grant W81XWH-15-1-0437.

Please address correspondence to Tracy Butler, MD, Weill Cornell Medicine, Brain Health Imaging Institute, 407 East 61st St, 2nd Floor, New York, NY 10065; e-mail: tab2006@med.cornell.edu

Indicates open access to non-subscribers at www.ajnr.org

Indicates article with online supplemental data.

<http://dx.doi.org/10.3174/ajnr.A7903>

vivo neuroimaging is relatively simple because of its vastly higher photon attenuation compared with water and brain, making it easily visible on CT.

For decades, CP calcification has been recognized as a normal phenomenon, with gradually increasing calcification noted with increasing age. CP calcification may have been the first age-related brain change ever detected in living humans. In 1930, Cornelius Dyke, considered the world's first neuroradiologist, noticed that CP calcification on skull radiographs was rare in children but common in the elderly.¹⁷ This finding was demonstrated in 1980 using CT.¹⁸ Markedly increased calcification of the CP, basal ganglia, and other brain structures in association with neuropsychiatric decline constitutes the still-poorly-understood and underdiagnosed syndrome of Fahr disease.¹⁹ CP calcification has received less research attention in recent years, in large part because MRI, with its submillimeter spatial resolution and lack of radiation has supplanted CT as the technique of choice for human neuroimaging research, and the variable signal of calcium on typical MRI makes calcium quantification on MRI challenging^{20,21} (though novel quantitative susceptibility mapping sequences under development may, in the future, support MRI quantification of calcium with an accuracy approaching that of CT²²).

To our knowledge, decades-old recognition of increasing CP calcification with aging and certain diseases has not been linked to the more recent understanding that CP has important roles beyond CSF production, in particular the regulation of neuroinflammation.¹⁻⁶ Neuroinflammation can currently be measured in vivo in humans using PET with radiotracers sensitive to the translocator protein (TSPO) expressed by activated microglia, the resident immune cell type of the brain.²³⁻²⁵ Increased regional TSPO PET signal has been demonstrated in a number of human neuroinflammatory and neurodegenerative disorders.^{23,25} However, despite the development of several new TSPO radiotracers during the past 15 years, there remain significant challenges associated with TSPO PET implementation, quantification, and interpretation, motivating research to identify additional biomarkers for neuroinflammation appropriate for human use.^{25,26} Intriguingly, 2 recent PET studies showed that cortical TSPO expression correlated with MRI-measured CP volume in patients with MS⁶ and depression.¹¹ On the basis of neuropathologic evidence that calcium deposition is associated with CP basement membrane thickening and fibrous stroma expansion in aging and disease,¹³⁻¹⁶ we wondered whether this correlation between CP volume and TSPO PET-measured neuroinflammation could be due to calcium. If so, CP calcium, which is easily detectable using CT, could represent a simple biomarker of neuroinflammation.

We, therefore, took a multimodal imaging approach, combining CT, MRI, and TSPO PET to measure the relationship between CP calcium and cortical neuroinflammation in a convenience sample of subjects (healthy controls and patients with Parkinson disease [PD]) who had undergone PET using the TSPO radiotracer ¹¹C-PK11195 (PK) at our institution and who had agreed to their data being included in a local neuroimage repository.

We developed an automated method for measuring CP calcium volume using low-dose CT (routinely acquired during PET/CT studies) and MRI, which we validated against semimanual tracing.

We hypothesized that the volume of calcium within the CP would be an independent predictor of PET-measured neuroinflammation.

Although the purpose of this study was to assess the contribution of CP calcium to cortical neuroinflammation as a general phenomenon, rather than as a function of disease, we also assessed the possible effects of the diagnosis (PD or control) on CP calcium, TSPO PET, and their interaction.

MATERIALS AND METHODS

Subjects

Subjects ($n = 60$) who underwent PK PET for several different studies conducted on a single PET/CT scanner between 2013 and 2019 were included in this analysis. This was a convenience sample based on available scan data. Subjects were either healthy controls ($n = 43$) or had been diagnosed with PD without dementia ($n = 17$) on the basis of standard criteria.²⁷ Most subjects with PD were taking ≥ 1 medication for PD. Healthy subjects were free from serious medical or neurologic disease including substance abuse. Common medical conditions in older subjects such as hypertension and hypercholesterolemia and medications to treat these conditions were not exclusionary. No subjects were taking anti-inflammatory medication. All subjects provided informed consent to participate in a disease-focused research study and for their data to be included in a registry for future analyses such as this one.

PET and MR Image Acquisition

PET images were acquired during 1 hour in list mode, starting at the time of injection of ~ 370 MBq of PK on a Biograph PET/CT scanner (Siemens) (voxel size: $1.0182 \times 1.0182 \times 2.025$ mm³). Low-dose CT was acquired immediately before the PET acquisition (voxel size: $0.488 \times 0.488 \times 1.5$ mm³). 3D volumetric T1-weighted BRAVO (GE Healthcare) (voxel size: $0.9375 \times 0.9375 \times 1.5$ mm³) or MPRAGE (voxel size: 1 mm³ isotropic) MR images were acquired using a Discovery MR750 (GE Healthcare) or Tim Trio 3T (Siemens) scanner, respectively.

PET Image Processing

PET images were reconstructed into 22 frames and motion-corrected using MCFLIRT²⁸ (<https://fsl.fmrib.ox.ac.uk/fsl/fslwiki/MCFLIRT>) in FSL (<http://www.fmrib.ox.ac.uk/fsl>).²⁹ Nondisplaceable binding potential (BPnd) images reflecting the concentration of TSPO expressed by activated microglia, irrespective of tracer delivery and blood flow, were generated from dynamic PET using a multilinear reference tissue model³⁰ implemented in the freely available software package FireVoxel (<https://firevoxel.org>). The reference tissue time-activity curve was identified via optimized supervised cluster analysis,³¹ which is considered the method of choice for analyzing PK PET scans.³²

MR Image Processing

FreeSurfer, Version 7 (<http://surfer.nmr.mgh.harvard.edu>),³³ was used to segment MR images for 3 purposes: to define the bilateral cortical ROI as well as other regions for quantifying PET signal; to segment the bilateral lateral ventricles for the automated calcium-quantification method described below; and to quantify CP and lateral ventricle volume to be included as predictors of cortical inflammation. For this latter purpose, CP and ventricular volumes

were divided by each subject's whole-brain volume, calculated using SPM 12 (<http://www.fil.ion.ucl.ac.uk/spm/software/spm12>), to account for head size. To quantify inflammation (average BPnd) over the cortical ROI, each subject's T1-weighted MRI was linearly coregistered to his or her summed PET image with rigid body transformation in FSL.²⁹ ROIs were transformed to PET space with the inverse transformation matrix from the coregistration step and eroded 1 mm in-plane to minimize partial volume effects.

Semimanual Quantification of CP Calcium on CT

Using FireVoxel, CT images were windowed at width = 100 Hounsfield units (HU) and level = 50 HU to clearly visualize CP calcifications, which typically have a signal of >100 HU.³⁴ 3D ROIs of CP calcification within all horns of the bilateral lateral ventricles were drawn using an electronic paint brush on contiguous axial images. ROIs were then thresholded at 60 HU to exclude any noncalcified voxels. Semimanual tracing was performed by one rater on a random subset of scans ($n = 44$).

Automated Quantification of CP Calcium Using MRI and CT

T1 MRI and FreeSurfer segmentations were coregistered to CT using rigid transformation with the Advanced Normalization Tools software package (<http://stnava.github.io/ANTs/>).³⁵ An ROI mask consisting of the bilateral CPs and the posterior portion of the bilateral lateral ventricles (posterior to the most anterior extent of the CP) was generated. Excluding the most anterior portion of this mask prevented erroneous misidentification of parenchymal voxels as calcified and was found to improve correlation with manual tracing. Voxels with Hounsfield units of >100 within this combined CP/posterior lateral ventricle mask were used as seeds to build a weighted image based on the intensity difference. This weighted image was segmented into background and foreground using the fast marching method.³⁶ Clusters from the segmentation were then divided into 2 groups using k-means clustering,³⁷ and the one with higher signal was selected as the calcified CP voxels.

Statistical Analyses

Analyses were performed in SPSS, Version 26 (IBM). Results were considered significant at $P < .05$.

Subject demographic factors were summarized using means and SDs. Although between-group differences were not the focus of this study, possible demographic differences between subjects with PD and controls were assessed using 2-sample t test (age) and χ^2 test (sex).

The intraclass correlation coefficient (ICC) assessed agreement between semimanual and automated CP calcium volumes.

Multiple linear regression was used to assess the contribution of CP calcium, CP overall volume, ventricle volume, age, sex, body mass index (BMI; previously shown to affect TSPO PET³⁸), and diagnosis (control or PD) to the dependent variable of cortical BPnd. Because disease effects on these measures are unknown, we also assessed whether the interaction between diagnosis and any of these variables contributed significantly to cortical BPnd.

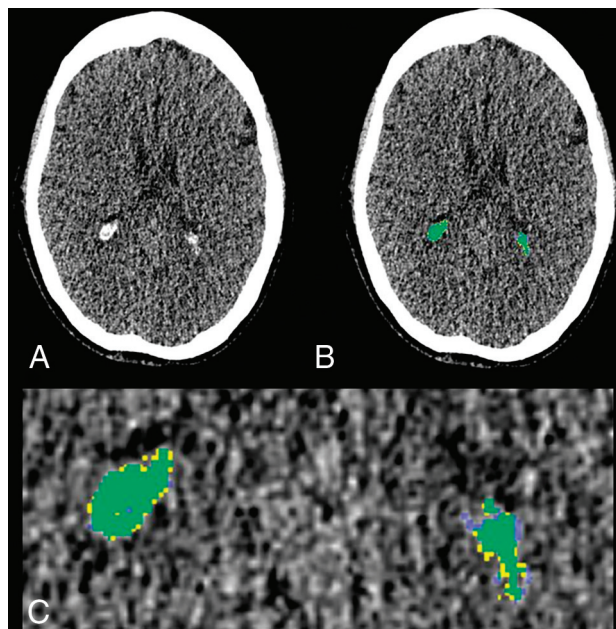


FIG 1. Example of CP calcification segmentation. A, Axial section from a low-dose CT acquired with PET/CT shows CP calcification in the occipital horn of the lateral ventricles bilaterally. B, Semimanually traced CP calcification is shown in yellow; fully-automated segmentation, in blue; and the overlap, in green. C, Magnified view of B shows close correspondence between semimanual and automated CP calcification segmentation.

In exploratory analyses using Mann-Whitney tests, we assessed whether any measured neuroimaging parameters differed between subjects with PD and controls.

RESULTS

Subject Demographics

Subjects ($n = 60$) ranged in age from 23 to 78 (mean, 57.0 [SD, 14.3]) years and included 24 (40%) women. The 2 types of subjects included in our convenience sample (PD [$n = 17$] and control [$n = 43$]) did not differ significantly by age, sex, or BMI. Details of subject demographics are presented in the Online Supplemental Data.

Comparison between Semimanual and Automated CP Calcium Measurements

There was excellent absolute agreement between semimanual and automated calcium measurements (ICC = 0.982, $F[43, 43] = 71.42$, $P < .001$). On the basis of this agreement, for all subsequent analyses, CP calcium refers to the automated value. Figure 1 shows an example of CP semimanual and automated segmentation.

Association of CP Calcium, CP Overall Volume, Ventricle Volume, Age, Sex, BMI, and Diagnosis with Cortical BPnd

A multiple regression model ($R^2 = 0.298$, adjusted $R^2 = 0.203$ $F[7, 52] = 3.15$, $P = .008$; details provided in the Table and Fig 2) showed that only age ($P = .017$) and CP calcium ($P = .017$) were significant predictors of cortical BPnd. Neither CP volume, ventricle volume, sex, nor diagnosis (control versus PD) was a

Linear regression model predicting cortical BPnd in 60 subjects^a

Variable	Unstandardized β	Standardized β	P Value
CP calcium volume	2.77E ⁻⁵	0.324	.017
Age	0.001	0.336	.017
CP volume	-1.78E ⁻⁵	-0.256	.181
Ventricle volume	4.97E ⁻⁷	0.219	.230
Sex	0.006	0.127	.310
BMI	-0.001	-0.145	.267
Diagnosis (control or PD)	0.002	0.041	.751

^aOnly CP calcium and age were significant predictors.

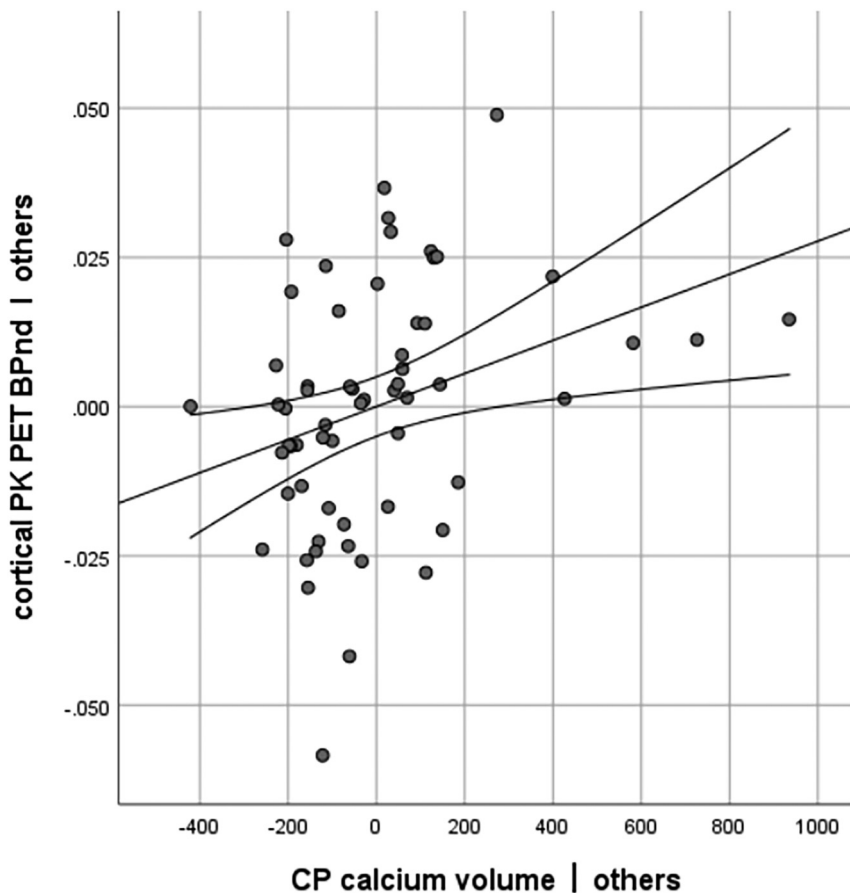


FIG 2. Partial regression plot showing the relation of CP calcium to PK BPnd in 60 subjects when controlling for the other variables (CP overall volume, ventricle volume, age, sex, BMI, and diagnosis [PD or control]).

significant predictor of cortical BPnd, and no interaction terms were significant.

Exploratory Group Differences

As shown in the Online Supplemental Data, there were no significant differences in the neuroimaging parameters of interest (CP calcium volume, CP overall volume, PK PET cortical BPnd) between subjects with PD and controls, though there was a nonsignificant trend ($P = .078$) for subjects with PD to have greater cortical BPnd than controls. BPnd in other brain regions also did not differ between subjects with PD and controls (all $P > .1$). These results are shown in the Online Supplemental Data, along with an example of a PK PET scan with normal findings illustrating typical regional TSPO expression.

DISCUSSION

We show that the volume of calcium within CP—but not CP overall volume—is associated with TSPO PET-measured cortical neuroinflammation and provides a method for accurately and automatically measuring CP calcium volume using MRI and low-dose CT. This method was highly congruent ($ICC = 0.98$) with the gold standard of manual tracing. We discuss implications of these findings as well as important limitations.

CP Calcification May Account for Prior Findings of CP Enlargement in Association with Neuroinflammatory Disease

Our results shed light on the basis of pathologic CP enlargement increasingly recognized in association with human inflammatory and neurodegenerative diseases.^{6-8,10,11} It is possible that unmeasured CP calcium can explain prior findings of CP enlargement in human aging and disease, including highly relevant recent findings of CP enlargement in association with TSPO PET-measured inflammation in MS and depression.^{6,11} Additional work, including studies linking in vivo or ex vivo neuroimaging of the human CP to direct tissue assessment, would be needed to determine more precisely the contribution of calcium and other CP histologic features to MRI-measured volume of the CP and its relation with neuroinflammation. It will also be important to determine whether our finding that CP calcification but not CP overall volume predicts cortical TSPO expression, which we have demonstrated in subjects without known neuroinflammatory disease, holds true in

subjects with more prominent neuroinflammation as occurs in MS.

CP Calcification as a Potential Biomarker for Neuroinflammation

Assessing neuroinflammation in humans is challenging, and current methods are limited to TSPO PET, which has well-known limitations, including a low SNR and poor availability outside academic medical centers.^{25,26} Our finding that CP calcification correlated significantly with cortical TSPO expression, coupled with our automated method for quantifying CP calcification using low-dose CT, suggests the potential for CP calcification to serve as a relatively easily acquired biomarker or proxy for neuroinflammation.

Because our results are based on a convenience sample of subjects and do not include subjects with overt neuroinflammatory disease, additional work would be needed to determine whether CP calcification correlates with TSPO PET in diseases associated with more severe neuroinflammation like MS. It would also be important to determine whether CP calcification changes in response to anti-inflammatory therapy. While brain calcium deposits are often considered permanent and life-long, a recent study using [¹⁸F]-NaF PET showed that the calcium in the CP may be uniquely metabolically active and potentially dynamic.³⁹ Furthermore, parenchymal calcification associated with neonatal toxoplasmosis has been shown to diminish with antimicrobial treatment.⁴⁰

CP Calcification Explains Interindividual Variability in TSPO PET

Wide and unexplained interindividual variability in TSPO PET is a known limitation of this technique, making detection of disease-specific alterations challenging.^{25,26} Our multiple regression model including age and CP calcium explained 30% of the variability in cortical TSPO expression. While this explanatory power may seem modest, it is similar to the effect of the TSPO gene *rs6971* polymorphism that defines high-, low-, and mixed-affinity binders in studies using second-generation TSPO PET tracers (but not studies like this one using the first-generation tracer PK).^{41,42} Studies using second-generation TSPO tracers must genetically screen all subjects because accounting for this polymorphism is essential for data interpretation. Similarly, accounting for CP calcification would be expected to reduce unexplained variability in TSPO PET studies, improving interpretability and facilitating detection of effects of interest.

No Significant Differences between Subjects with PD and Controls

Although not the focus of this study, in exploratory analyses, we assessed CP calcification, CP volume, and cortical neuroinflammation in subjects with PD compared with controls and did not find any significant differences. Normal CP volume in PD is in accord with 1 prior study.⁸ There was a trend ($P = .078$) for subjects with PD to have greater cortical TSPO expression than controls. Prior TSPO PET studies of PD have provided variable results: Some show increased TSPO expression in regions including the cortex, basal ganglia, and midbrain compared with controls,^{43,44} though others show no significant differences.⁴⁵ Current negative results in this relatively small sample of subjects with PD cannot resolve the controversy over this issue. Our finding that subject diagnosis did not affect the correlation between CP calcification and cortical neuroinflammation suggests that this correlation may be a general phenomenon, potentially broadly relevant in human health and disease. Additional work in larger and more diagnostically diverse groups of subjects is needed.

Usefulness of Low-Dose CT Acquired with PET to Measure CP Calcification

Because most human PET studies are currently performed using PET/CT machines, an association of CP calcification with any type of PET-measured molecular information can be assessed with no additional cost or radiation exposure. For example, CP dysfunction

has been posited to play an early etiologic role in AD.⁷⁻⁹ Whether CP calcification predicts AD protein deposition could be assessed using existing longitudinal neuroimage repositories if the CT portion of the PET/CT were recognized as valuable and made available.

Limitations

This study has several important limitations.

This is a cross-sectional study demonstrating a correlation between CP calcification and cortical neuroinflammation. Results suggest that CP calcification, which is simple to measure, could serve as a biomarker for cortical inflammation, which is much more difficult to measure. However, this study cannot clarify causality, the mechanism linking these 2 measures, nor whether increased cortical TSPO expression may be detrimental or beneficial. While PET-measured TSPO expression has traditionally been considered to reflect an activated, proinflammatory, detrimental microglial phenotype termed M2 (versus a resting M1 phenotype associated with the maintenance of homeostasis), it is now recognized that this bimodal scheme is an oversimplification and that microglial phenotypes and functions cannot be fully characterized using a probe for a single molecule.⁴⁶ A recent study using an animal model of Fahr disease found that activated microglia were beneficial in regulating calcification and preventing neurodegeneration.⁴⁷ The question of whether such homeostatic interplay between microglia and calcification occurs in humans and whether it may be altered in diseases such as MS and AD associated with microglial dysfunction^{1-6,48} requires additional longitudinal study.

Another limitation of this study is that TSPO is expressed in the brain not just by microglia but by several cell types including other brain macrophages, astrocytes, vascular endothelial cells, and possibly neurons.^{24,49,50} Meningeal macrophages⁵¹ bordering the cortical ROI in this study may contribute to the cortical signal. Because of these limitations of TSPO PET imaging, there is intense interest in identifying new neuroimaging methods to quantify neuroinflammation in vivo in humans.²⁴⁻²⁶ However, currently, TSPO PET remains the only available research option, and we apply optimal image processing and analysis methods in this study.³²

It is a limitation that our analysis is retrospective and based on a relatively small convenience sample of heterogeneous subjects (controls and subjects with PD) scanned for different projects and that we did not include subjects with a definite neuroinflammatory disease like MS. Future prospective studies including additional patient populations are needed to determine whether the association of CP calcification with cortical TSPO expression that we have demonstrated holds true when the range of neuroinflammation across subjects is greater. Replication and extension of our findings in greater numbers of subjects and in different disease states is necessary and would be facilitated by the inclusion of the CT portion of PET/CT studies in public neuroimage repositories. Our results show that information about CP calcification present in low-dose CT is valuable and should not be discarded.

CONCLUSIONS

CP calcification volume can be reliably quantified using semianual tracing on low-dose CT acquired with PET/CT and fully

automatically using our new, accurate (ICC with semimanual tracing = 0.98) CT/MRI method. CP calcification and age—but not overall CP volume—significantly predicted PK PET-measured cortical neuroinflammation in this study. CP calcification is a relatively easily assessed, previously overlooked potential biomarker for neuroinflammation and CP pathology.

ACKNOWLEDGMENT

We are grateful to Steve Poulin, PhD, for assistance with statistical analyses.

Disclosure forms provided by the authors are available with the full text and PDF of this article at www.ajnr.org.

REFERENCES

1. Reboldi A, Coisne C, Baumjohann D, et al. **C-C chemokine receptor 6-regulated entry of TH-17 cells into the CNS through the choroid plexus is required for the initiation of EAE.** *Nat Immunol* 2009;10:514–23 [CrossRef Medline](#)
2. Kunis G, Baruch K, Rosenzweig N, et al. **IFN- γ -dependent activation of the brain's choroid plexus for CNS immune surveillance and repair.** *Brain* 2013;136:3427–40 [CrossRef Medline](#)
3. Schwartz M, Baruch K. **The resolution of neuroinflammation in neurodegeneration: leukocyte recruitment via the choroid plexus.** *EMBO J* 2014;33:7–22 [CrossRef Medline](#)
4. Manouchehri N, Stuve O. **Choroid plexus volumetrics and brain inflammation in multiple sclerosis.** *Proc Natl Acad Sci U S A* 2021;118:e2115221118 [CrossRef Medline](#)
5. Fleischer V, Gonzalez-Escamilla G, Ciolac D, et al. **Translational value of choroid plexus imaging for tracking neuroinflammation in mice and humans.** *Proc Natl Acad Sci U S A* 2021;118:e2025000118 [CrossRef Medline](#)
6. Ricigliano VA, Morena E, Colombi A, et al. **Choroid plexus enlargement in inflammatory multiple sclerosis: 3.0-T MRI and translocator protein PET evaluation.** *Radiology* 2021;301:166–77 [CrossRef Medline](#)
7. Choi JD, Moon Y, Kim HJ, et al. **Choroid plexus volume and permeability at brain MRI within the Alzheimer disease clinical spectrum.** *Radiology* 2022;304:635–45 [CrossRef Medline](#)
8. Tadayon E, Pascual-Leone A, Press D, et al; Alzheimer's Disease Neuroimaging Initiative. **Choroid plexus volume is associated with levels of CSF proteins: relevance for Alzheimer's and Parkinson's disease.** *Neurobiol Aging* 2020;89:108–17 [CrossRef Medline](#)
9. Alvira-Botero X, Carro EM. **Clearance of amyloid-beta peptide across the choroid plexus in Alzheimer's disease.** *Curr Aging Sci* 2010;3:219–29 [CrossRef Medline](#)
10. Alisch JS, Kiely M, Triebswetter C, et al. **Characterization of age-related differences in the human choroid plexus volume, microstructural integrity, and blood perfusion using multiparameter magnetic resonance imaging.** *Front Aging Neurosci* 2021;13:734992 [CrossRef Medline](#)
11. Althubaity N, Schubert J, Martins D, et al. **Choroid plexus enlargement is associated with neuroinflammation and reduction of blood brain barrier permeability in depression.** *Neuroimage Clin* 2022;33:102926 [CrossRef Medline](#)
12. Egorova N, Gottlieb E, Khlif MS, et al. **Choroid plexus volume after stroke.** *Int J Stroke* 2019;14:923–30 [CrossRef Medline](#)
13. Živković VS, Stanojković MM, Antić MM. **Psammoma bodies as signs of choroid plexus ageing: a morphometric analysis.** *Vojnosanitetski Pregled* 2017;74:1054–59 [CrossRef](#)
14. Alcolado JC, Moore IE, Weller RO. **Calcification in the human choroid plexus, meningiomas and pineal gland.** *Neuropathol Appl Neurobiol* 1986;12:235–50 [CrossRef Medline](#)
15. Wolburg H, Paulus W. **Choroid plexus: biology and pathology.** *Acta Neuropathol* 2010;119:75–88 [CrossRef Medline](#)
16. Emerich DF, Skinner SJ, Borlongan CV, et al. **The choroid plexus in the rise, fall and repair of the brain.** *Bioessays* 2005;27:262–74 [CrossRef Medline](#)
17. Dyke CG. **Indirect signs of brain tumor as noted in routine roentgen examinations: displacement of the pineal shadow (a survey of 3000 consecutive skull examinations).** *AJR Am J Roentgenol* 1930;23:598–606
18. Modic M, Weinstein M, Rothner A, et al. **Calcification of the choroid plexus visualized by computed tomography.** *Radiology* 1980;135:369–72 [CrossRef Medline](#)
19. Nicolas G, Charbonnier C, Campion D, et al. **Estimation of minimal disease prevalence from population genomic data: application to primary familial brain calcification.** *Am J Med Genet B Neuropsychiatr Genet* 2018;177:68–74 [CrossRef Medline](#)
20. Adams LC, Bresslem K, Böker SM, et al. **Diagnostic performance of susceptibility-weighted magnetic resonance imaging for the detection of calcifications: a systematic review and meta-analysis.** *Sci Rep* 2017;7:15506 [CrossRef Medline](#)
21. Wehrli FW. **Magnetic resonance of calcified tissues.** *J Magn Reson* 2013;229:35–48 [CrossRef Medline](#)
22. Wen Y, Spincemaille P, Nguyen T, et al. **Multiecho complex total field inversion method (mcTFI) for improved signal modeling in quantitative susceptibility mapping.** *Magn Reson Med* 2021;86:2165–78 [CrossRef Medline](#)
23. Kreisl WC, Kim MJ, Coughlin JM, et al. **PET imaging of neuroinflammation in neurological disorders.** *Lancet Neurol* 2020;19:940–50 [CrossRef Medline](#)
24. Guilarte TR, Rodichkin AN, McGlothlan JL, et al. **Imaging neuroinflammation with TSPO: a new perspective on the cellular sources and subcellular localization.** *Pharmacol Ther* 2022;234:108048 [CrossRef Medline](#)
25. Jain P, Chaney AM, Carlson ML, et al. **Neuroinflammation PET imaging: current opinion and future directions.** *J Nucl Med* 2020;61:1107–12 [CrossRef Medline](#)
26. Janssen B, Vugts DJ, Windhorst AD, et al. **PET imaging of microglial activation: beyond targeting TSPO.** *Molecules* 2018;23:607 [CrossRef Medline](#)
27. Hughes AJ, Daniel SE, Kilford L, et al. **Accuracy of clinical diagnosis of idiopathic Parkinson's disease: a clinico-pathological study of 100 cases.** *J Neurol Neurosurg Psychiatry* 1992;55:181–84 [CrossRef Medline](#)
28. Jenkinson M, Bannister P, Brady M, et al. **Improved optimization for the robust and accurate linear registration and motion correction of brain images.** *Neuroimage* 2002;17:825–41 [CrossRef Medline](#)
29. Smith SM, Jenkinson M, Woolrich MW, et al. **Advances in functional and structural MR image analysis and implementation as FSL.** *Neuroimage* 2004;23:S208–19 [CrossRef Medline](#)
30. Butler T, Li Y, Tsui W, et al. **Transient and chronic seizure-induced inflammation in human focal epilepsy.** *Epilepsia* 2016;57:e191–94 [CrossRef Medline](#)
31. Schubert J, Tonietto M, Turkheimer F, et al. **Supervised clustering for TSPO PET imaging.** *Eur J Nucl Med Mol Imaging* 2021;49:257–68 [CrossRef Medline](#)
32. Wimberley C, Lavis S, Hillmer A, et al. **Kinetic modeling and parameter estimation of TSPO PET imaging in the human brain.** *Eur J Nucl Med Mol Imaging* 2021;49:246–56 [CrossRef Medline](#)
33. Fischl B, Salat DH, Busa E, et al. **Whole brain segmentation: automated labeling of neuroanatomical structures in the human brain.** *Neuron* 2002;33:341–55 [CrossRef Medline](#)
34. Yalcin A, Ceylan M, Bayraktutan OF, et al. **Age and gender related prevalence of intracranial calcifications in CT imaging: data from 12,000 healthy subjects.** *J Chem Neuroanat* 2016;78:20–24 [CrossRef Medline](#)
35. Avants BB, Tustison NJ, Song G, et al. **A reproducible evaluation of ANTs similarity metric performance in brain image registration.** *Neuroimage* 2011;54:2033–44 [CrossRef Medline](#)

36. Sethian JA. *Level Set Methods and Fast Marching Methods: Evolving interfaces in computational geometry, fluid mechanics, computer vision, and materials science*. Cambridge University Press; 1999
37. Arthur D, Vassilvitskii S. **k-means++ the advantages of careful seeding**. Proceedings of the eighteenth annual ACM-SIAM symposium on Discrete algorithms (2007, January, pp 1027–1035).
38. Tuisku J, Plavén-Sigraý P, Gaiser EC, et al; HRRT [¹¹C] PBR28 Study Group. **Effects of age, BMI and sex on the glial cell marker TSPO: a multicentre [¹¹C] PBR28 HRRT PET study**. *Eur J Nucl Med Mol Imaging* 2019;46:2329–38 [CrossRef Medline](#)
39. Al-Zaghal A, Seraj SM, Werner TJ, et al. **Assessment of physiologic intracranial calcification in healthy adults using 18F-NaF PET/CT**. *J Nucl Med* 2018 Jul 12. [Epub ahead of print] [CrossRef](#)
40. Patel DV, Holfels EM, Vogel NP, et al. **Resolution of intracranial calcifications in infants with treated congenital toxoplasmosis**. *Radiology* 1996;199:433–40 [CrossRef Medline](#)
41. Suridjan I, Rusjan P, Voineskos AN, et al. **Neuroinflammation in healthy aging: a PET study using a novel translocator protein 18 kDa (TSPO) radioligand, [18F]-FEPPA**. *Neuroimage* 2014;84:868–75 [CrossRef Medline](#)
42. Owen DR, Yeo AJ, Gunn RN, et al. **An 18-kDa translocator protein (TSPO) polymorphism explains differences in binding affinity of the PET radioligand PBR28**. *J Cereb Blood Flow Metab* 2012;32:1–5 [CrossRef Medline](#)
43. Gerhard A. **TSPO imaging in parkinsonian disorders**. *Clin Transl Imaging* 2016;4:183–90 [CrossRef Medline](#)
44. Zhang PF, Gao F. **Neuroinflammation in Parkinson's disease: a meta-analysis of PET imaging studies**. *J Neurol* 2022;269:2304–14 [CrossRef Medline](#)
45. Ghadery C, Koshimori Y, Coakeley S, et al. **Microglial activation in Parkinson's disease using [18 F]-FEPPA**. *J Neuroinflammation* 2017;14:8 [CrossRef Medline](#)
46. Salter MW, Stevens B. **Microglia emerge as central players in brain disease**. *Nat Med* 2017;23:1018–27 [CrossRef Medline](#)
47. Zarb Y, Sridhar S, Nassiri S, et al. **Microglia control small vessel calcification via TREM2**. *Sci Adv* 2021;7:eabc4898 [CrossRef Medline](#)
48. Hansen DV, Hanson JE, Sheng M. **Microglia in Alzheimer's disease**. *J Cell Biol* 2018;217:459–72 [CrossRef Medline](#)
49. Gui Y, Marks JD, Das S, et al. **Characterization of the 18 kDa translocator protein (TSPO) expression in post-mortem normal and Alzheimer's disease brains**. *Brain Pathol* 2020;30:151–64 [CrossRef Medline](#)
50. Notter T, Schalbetter SM, Clifton NE, et al. **Neuronal activity increases translocator protein (TSPO) levels**. *Mol Psychiatry* 2021;26:2025–37 [CrossRef Medline](#)
51. Mildemberger W, Stifter SA, Greter M. **Diversity and function of brain-associated macrophages**. *Curr Opin Immunol* 2022;76:102181 [CrossRef Medline](#)